Femtosecond Dynamics of Momentum-Dependent Magnetic Excitations from Resonant Inelastic X-Ray Scattering in $CaCu_2O_3$

Valentina Bisogni,[1,2,*] Stefanos Kourtis,[1] Claude Monney,[2,3,†] Kejin Zhou,[2,‡] Roberto Kraus,[1] Chinnathambi Sekar,[1,§] Vladimir Strocov,[2] Bernd Büchner,[1,4] Jeroen van den Brink,[1,4] Lucio Braicovich,[5] Thorsten Schmitt,[2] Maria Daghofer,[1] and Jochen Geck[1]

[1]*Leibniz Institute for Solid State and Materials Research IFW Dresden, 01069 Dresden, Germany*
[2]*Research Department Synchrotron Radiation and Nanotechnology, Paul Scherrer Institut, CH-5232 Villigen PSI, Switzerland*
[3]*Fritz-Haber-Institut der Max-Planck-Gesellschaft, Faradayweg 4-6, 14195 Berlin, Germany*
[4]*Department of Physics, Technical University Dresden, D-1062 Dresden, Germany*
[5]*CNR/SPIN, CNISM, and Dipartimento di Fisica, Politecnico di Milano, Piazza Leonardo da Vinci 32, 20133 Milano, Italy*

(Received 31 July 2013; revised manuscript received 27 January 2014; published 7 April 2014)

Taking spinon excitations in the quantum antiferromagnet $CaCu_2O_3$ as an example, we demonstrate that femtosecond dynamics of magnetic electronic excitations can be probed by direct resonant inelastic x-ray scattering (RIXS). To this end, we isolate the contributions of single and double spin-flip excitations in experimental RIXS spectra, identify the physical mechanisms that cause them, and determine their respective time scales. By comparing theory and experiment, we find that double spin flips need a finite amount of time to be generated, rendering them sensitive to the core-hole lifetime, whereas single spin flips are, to a very good approximation, independent of it. This shows that RIXS can grant access to time-domain dynamics of excitations and illustrates how RIXS experiments can distinguish between excitations in correlated electron systems based on their different time dependence.

DOI: 10.1103/PhysRevLett.112.147401 PACS numbers: 78.70.Ck, 75.30.Ds, 78.20.Ls, 78.47.J-

Traditional spectroscopic methods used in condensed matter experiments relate dynamical properties of a material to frequency-dependent correlation functions. These techniques have been very successful in probing elementary excitations of solids, revealing their sometimes unconventional nature. For instance, using frequency-resolved spectroscopies to study low-dimensional cuprates, electronic quasiparticles that are fractions of an electron, in the sense that they carry either its spin, charge, or orbital, have been detected [1–3].

Technological advances in intense pulsed radiation sources, including those at novel x-ray free electron laser (XFEL) facilities [4], nowadays enable us to observe dynamics via time-resolved measurements. A usual scheme is to first excite a system using a pump pulse and then to probe the excited state at a later time by means of a probe pulse. Today, these pump-probe experiments allow studying the temporal evolution of excited states in the pico-, femto-, and attosecond time scales [5–7]. The pump-probe approach provides opportunities for further exploration of correlated electron materials, because the femtosecond to picosecond range corresponds to dynamics usually determined by electron-electron or electron-phonon interactions—processes of key importance for the physical properties of these materials.

A conceptually alternative route for the time domain is core-level spectroscopy, either involving outgoing electrons [8] or photons [9–12]. Initially, a core electron is promoted into an unoccupied orbital and an intermediate perturbed state with a finite lifetime, the core-hole lifetime τ, is created. At an average time τ after the core-hole creation, an electron decays into the core hole leading to emission of a photoelectron, Auger electron, or x-ray photon. The measured signal carries information on the generation and evolution of excitations created during the core-hole lifetime. In the case of L edges of $3d$ transition metals, the $2p$ core-hole lifetime is in the femtosecond range, corresponding to the dynamics of correlated electrons. Such a time scale accessible by core-level spectroscopy is still today much faster than that achievable by state of the art XFEL.

Resonant inelastic x-ray scattering (RIXS) is a photon-in—photon-out technique, which involves the creation of a core hole in the intermediate state and, therefore, implements the aforementioned core-hole clock. In addition, high-resolution RIXS is a unique technique for probing magnetic, orbital, and charge excitations in strongly correlated materials, often in the momentum resolved mode [3,13–19]. The combination of these properties makes RIXS a unique tool giving dynamical information. Besides being interesting *per se*, this approach allows us to disentangle excitations not well separated in energy and momentum by exploiting their different time scales as shown here. For all these reasons, the RIXS dynamics is potentially interesting for a variety of fields in solid state physics, and it is timely to investigate this option since RIXS is rapidly developing.

In this Letter, we demonstrate how the temporal evolution of electronic excitations during the core-hole lifetime leaves its fingerprint on the RIXS cross section. As an

example, we consider the elementary magnetic excitations of the spin chains in $CaCu_2O_3$. Via Cu L-edge RIXS, we measure two types of magnetic excitations in this material, which correspond to a single spin flip with a total spin change of $\Delta S = 1$ (S_1) and a double spin flip with $\Delta S = 0$ (S_0) [15,16,20–22]. Following a previously established approach [22], we extract the S_0 and S_1 contributions from the experimental spectra and compare the result to the theoretical RIXS response obtained by an exact-diagonalization simulation of the time dependence of the RIXS process in a 1D $S = 1/2$ chain. We show that the S_0 and S_1 excitations evolve on very different time scales and, therefore, contribute differently to the measured RIXS signal. Specifically, we establish that the S_1 part, which depends on strong spin-orbit coupling, is created mainly upon decay and is affected only slightly by the core-hole lifetime. Whereas the S_0 part takes a significantly long time to be created—its intrinsic time constant is $\tau_{S_0} = \hbar/J$, where J is the spin-spin interaction strength—and depends crucially on the intermediate state dynamics, the ratio of core-hole lifetime τ to τ_{S_0} determines, in fact, the S_0 contribution to the spectra.

The RIXS experiment was performed at the ADRESS beam line of the Swiss Light Source at the Paul Scherrer Institut [23], using the SAXES spectrometer [24]. The experimental layout is illustrated in Fig. 1(a). The energy of the incoming x-ray photons was tuned to the maximum of the Cu L_3 x-ray absorption peak at 931.5 eV [cf. Fig. 1(b)], for both linear in-plane (π) and out-of-plane (σ) polarizations ϵ. The combined energy resolution at this edge was 130 meV.

$CaCu_2O_3$ single crystals were grown as described in Ref. [25]. This material realizes a two-leg spin-1/2 ladder, as illustrated in Fig. 1(c). An important feature of this particular ladder structure is the 123° bond angle along the rung direction a, which results in anisotropic exchange constants $J_{\text{leg}} \simeq 10 \times J_{\text{rung}} \simeq 140$–$160$ meV [2,26]. Therefore, the two-leg ladders can be approximated as two weakly coupled spin-1/2 chains, since the effects of the coupling along the rung direction become important only at energies below 10 meV [2].

In the following, we focus on the magnetic RIXS excitations at energies between 100 and 300 meV where the effects of J_{rung} play no role. The corresponding experimental RIXS spectra for different momentum transfers q are shown in Fig. 1(d) as a vertical stack with q ranging between -1 to 1 (in units of π/b, where $b = 4.1$ Å) and for σ- (black) and π- (red) incoming polarized light. Already, from the raw data, the dispersion of the magnetic excitations is very clear. As can be seen in Fig. 1(e), the peak position tracks the lower bound of the two-spinon excitations and reaches a maximum at $q \simeq 0.5$. In addition to this, our RIXS data reveal the continuum of two-spinon excitations at higher energies above the lower bound. This is exactly what is expected for a spin-1/2 chain [27] and agrees very well with previous inelastic neutron scattering data [2,28]. Thus, we ascertain that, within the energy range

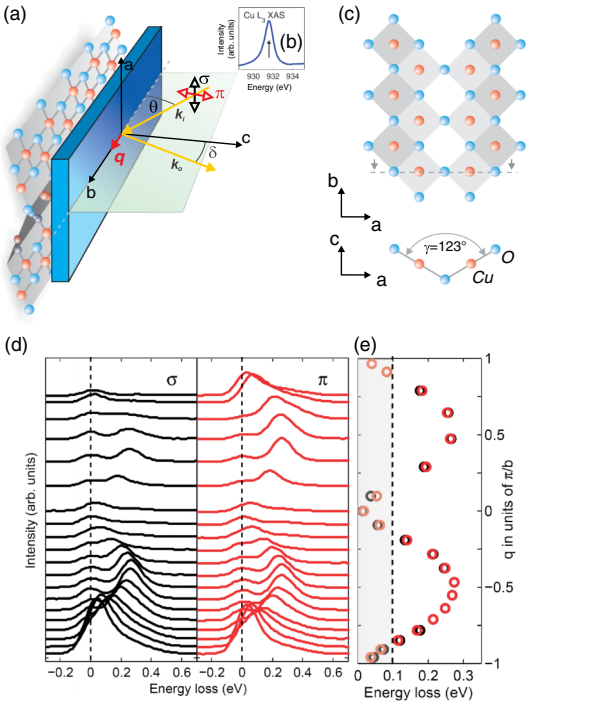

FIG. 1 (color online). (a) Experimental layout for the RIXS measurements. The scattering angle was set to 130°. (b) X-ray absorption (XAS) at Cu L_3 edge of $CaCu_2O_3$. (c) $CaCu_2O_3$ structure in the ab and ac planes. (d) RIXS spectra of $CaCu_2O_3$ for σ (black) and π (red) incoming polarized light, after being normalized to the dd area, between 1.3 and 2.8 eV (not shown here). The vertical offset between two consecutive spectra is proportional to the difference of the corresponding momenta [given by the y scale of panel (e)]. (e) Dispersion of the magnetic peak for the two polarizations (same color code). All the data have been measured at 40 K, above the Néel transition of $CaCu_2O_3$ ($T_N = 25$ K) [2].

accessed by the present RIXS experiment, the magnetic excitations of $CaCu_2O_3$ correspond to two-spinon excitations of antiferromagnetic (AFM) spin-1/2 chains with a superexchange $J \approx 160$ meV.

Figure 2 provides a schematic illustration of the dominant mechanisms, by which Cu L_3-edge RIXS creates two-spinon excitations in an AFM spin-1/2 chain. Initially, at $t = 0$, a $2p$ core electron is excited into the $3d$ valence shell [see Fig. 2(b)]. During the lifetime τ of the created core hole, two different processes can occur that leave magnetic excitations behind. (i) Because of spin-orbit coupling to the $2p$ state the core-hole spin can flip [Fig. 2(c), right panel]. After the core-hole decay, this results in a local spin flip in the valence shell of the excited site [Fig. 2(d), right panel], yielding the S_1 excitation. (ii) Two spins next to the core-hole site scatter at the doubly occupied site [Fig. 2(c), left panel]. After the decay of the core-hole state, again, two spinons have been created [Fig. 2(d), left panel], but this time the spinons have opposite spins, and hence, the total spin did not change. This is the S_0 process.

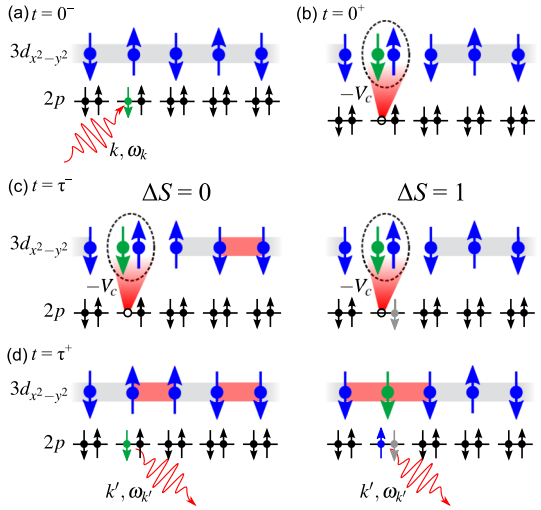

FIG. 2 (color online). Direct magnetic RIXS processes. (a) Schematic representation of the initial state $2p^6 3d^9$, i.e., the ground state of a 1D AFM $S = 1/2$ chain, at time $t = 0^-$ just before the creation of the core hole. (b) Intermediate state with one doublon and one core hole present ($2p^5 3d^{10}$ configuration) right after the creation of the core hole at $t = 0^+$. As the $3d$ level at the core-hole site is doubly occupied and has a net spin of 0, magnetic coupling to neighboring sites vanishes. (c) Intermediate state at a later time $t = \tau^-$, just before the deexcitation of the core hole. On the left side, two spins next to the core-hole site have flipped due to scattering on the doubly occupied site, i.e., the "cut" in the spin chain. On the right side, spin-orbit coupling of the $2p$ state has flipped the core-hole spin. The intermediate state doublon is subject to the core-hole potential V_c. (d) The two-spinon excitations (red bonds) in the final state at $t = \tau^+$. In (c) and (d), the left (right) part illustrates the S_0 (S_1) process.

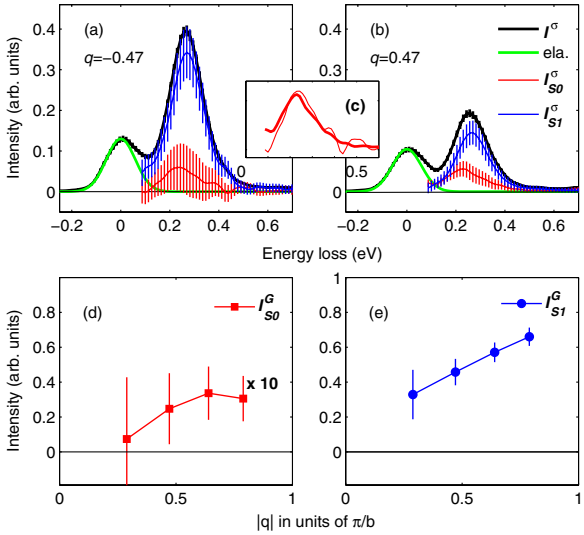

FIG. 3 (color online). (a) [(b)] Spectral decomposition of total RIXS intensity I^σ (black dotted line) into S_0 (red line) and S_1 (blue line) components for $q = -0.47$ ($q = 0.47$). The elastic signal is shown in green. (c) Comparison between the extracted I_{S_0} spectral shapes at $q = -0.47$ (thin line) and $q = 0.47$ (thick line). (d) [(e)] $I^G_{S_0}$ ($I^G_{S_1}$) as a function of q, estimated by integrating G_{S_0} (G_{S_1}) between 0.1 and 0.6 eV. Only positive q data are considered [32].

For a specific polarization ϵ, the magnetic RIXS intensity can be expressed as $I^\epsilon(q,\omega,\tau) = I^\epsilon_{S_0}(q,\omega,\tau) + I^\epsilon_{S_1}(q,\omega,\tau)$. To quantify these observations, we use the factorization introduced in Refs. [20,29], where $I^\epsilon_{S_0(S_1)}(q,\omega,\tau)$ can be written as $F^\epsilon_{S_0(S_1)}(q) G_{S_0(S_1)}(|q|,\omega,\tau)$, F being a local form factors depending on the geometrical parameters ϵ, q and corresponding to the transition between spin-orbit split $2p_{3/2}$ states to $3d_{x^2-y^2}$ state, while G are ground-state dynamical structure factors depending on energy transfer ω, magnitude of momentum transfer $|q|$ and—most importantly for the present analysis—core-hole lifetime τ. Following Refs. [20,30], $F^\epsilon_{S_1}$ is replaced by the local spin-flip probability $P^\epsilon_{\rm sf}$. Additionally, we assign to $F^\epsilon_{S_0}$ the elastic probability $P^\epsilon_{\rm el}$, because the state of the excited site has not changed during the S_0 process. The overall magnetic RIXS intensity is, thus, given by

$$I^\epsilon(q,\omega,\tau) = P^\epsilon_{\rm el}(q) G_{S_0}(|q|,\omega,\tau) + P^\epsilon_{\rm sf}(q) G_{S_1}(|q|,\omega,\tau). \quad (1)$$

The probabilities $P^\epsilon_{\rm el}(q)$ and $P^\epsilon_{\rm sf}(q)$ can be evaluated within the single ion model [31,32]. Considering the set of Eq. (1) for $\epsilon = \sigma$, π at a given q, with $I^\sigma(q,\omega,\tau)$ and $I^\pi(q,\omega,\tau)$ known from the experiment, it is possible to determine first, $G_{S_0}(|q|,\omega,\tau)$ and $G_{S_1}(|q|,\omega,\tau)$, not depending on ϵ, and second, to extract $I^\epsilon_{S_0}(q,\omega,\tau)$ and $I^\epsilon_{S_1}(q,\omega,\tau)$. Representative results of this analysis are given in Fig. 3. In panels 3(a) and 3(b), RIXS spectra taken at $q = -0.47$ and $q = 0.47$ with $\epsilon = \sigma$ are shown as well as their decomposition into $I^\sigma_{S_1}$ (blue) and $I^\sigma_{S_0}$ (red). The extracted S_0 and S_1 contributions at a given q show a large energy overlap, in qualitative agreement with theoretical expectations [21,33,34]. By comparing the independent results for the two q values, it can be seen that the energy position of each magnetic component coincides for $\pm q$, as demonstrated in Fig. 3(c) for the S_0 case. This strongly supports the validity of our decomposition analysis, as it correctly yields $G_{S_0,S_1} = G_{S_0,S_1}(|q|)$, without incorporating this as a condition.

The analysis also yields the ground-state dynamical structure factors G_{S_0} and G_{S_1}. Their integrated spectral weights as a function of $|q|$, $I^G_{S_0}$ and $I^G_{S_1}$, are shown in Figs. 3(d) and 3(e), respectively. Interestingly, the integrated spectral weights display different behaviors: while that of the S_0 component has a broad maximum around $q = 0.6$, the S_1 part increases steadily with q. Furthermore, depending on q, the S_0 contribution is roughly 10 to 20 times weaker in strength than S_1.

We now turn to the theoretical modeling of the time evolution of magnetic excitations in a spin-1/2 chain and its relation to the RIXS cross section. The effect of the core-hole lifetime τ on the RIXS process was simulated using exact diagonalization [21] for a ring of up to 16 sites modeling the $3d$ valence states and a time-dependent term describing the core hole

$$\mathcal{H}(t) = \mathcal{H}_{3d} + \Theta(t)\Theta(\tau - t)\mathcal{H}_{\rm corehole}. \quad (2)$$

$\mathcal{H}_{\text{corehole}}$ consists of a local attractive potential at a single site, which is switched on (at $t = 0$) and off (at $t = \tau$) together with the creation and annihilation of the extra d electron, respectively (see the illustration in Fig. 2). The effective spin flip in the S_1 process, see Fig. 2(c), is incorporated by creating and annihilating electrons with opposite spin in the $3d_{x^2-y^2}$ orbital at the core-hole site. Note that the core-hole lifetime $\tau = \hbar/\Gamma$, Γ being the core-hole lifetime broadening, is explicitly taken into account in both the S_0 and S_1 cases [32].

We compared several microscopic models of $\mathcal{H}_{3d}$, modeling the $3d_{x^2-y^2}$ chain with Hubbard, t-J, and Heisenberg models. In the former two, the doubly occupied site (doublon) is in principle allowed to move away from the core hole during the RIXS process, but for the experimentally determined core-hole potential V_c in cuprate materials of 9 eV [35], the doublon hopping was found to play no role [32]. Also, as long as $V_c \gtrsim U$, where U is the actual or implied on-site Coulomb repulsion in the model, the actual value of V_c does not significantly affect the direct RIXS process [21,32]. Thus, the only relevant aspect for creating the S_0 excitations turns out to be the vanishing spin of the doubly occupied site, which cuts the $S = 1/2$ chain. In the following, therefore, we will present results obtained by using a Heisenberg Hamiltonian, whose only energy scale J defines the spinon-propagation time scale $\tau_{S_0} = \hbar/J \approx 4fs$ ($J = 0.16$ eV for $CaCu_2O_3$).

From Figs. 4(a) and 4(b), it can be seen that the theoretical results for $I^G_{S_0}$ and $I^G_{S_1}$ closely follow the dispersive trends of the experimental findings shown in Figs. 3(d) and 3(e). Comparison to Bethe ansatz results from Ref. [34] [black dashed lines in Figs. 4(a) and (4b)] shows that finite-size effects are small. By increasing the lifetime τ, the calculated $I^G_{S_0}$ strongly increases [Fig. 4(a)], while the $I^G_{S_1}$ remains almost unchanged [21,33] [Fig. 4(b)]. This behavior is expected, since the spin flip in the S_1 process is directly introduced upon the decay and, therefore, dominates the response, while perturbative effects due to the intermediate-state doublon contribute only minutely to $I^G_{S_1}$. On the contrary, S_0 excitations are created only due to the presence of the intermediate state doublon. During the time span τ, excitations are generated at and propagate away from the core-hole site. Therefore, $I^G_{S_0}$ increases strongly with increasing τ and becomes significant only for $\tau \sim \hbar/J$. S_1 excitations, on the other hand, can occur even for $\tau \ll \hbar/J$.

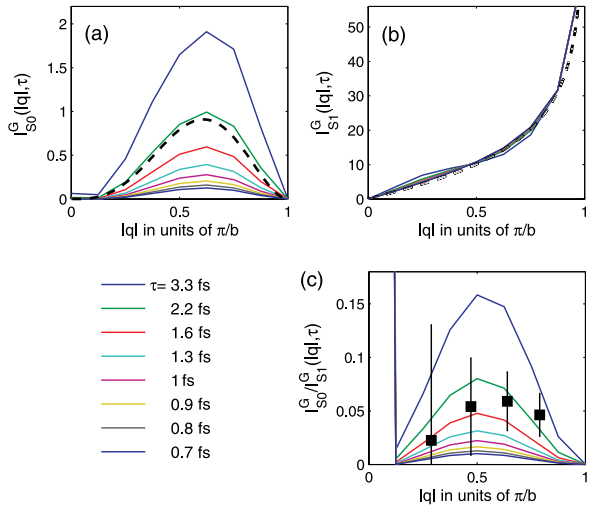

FIG. 4 (color online). Theoretical magnetic RIXS response and comparison to experiment. (a) [(b)] Numerically obtained $I^G_{S_0}(|q|)$ [$I^G_{S_1}(|q|)$] as a function of τ, calculated with exact diagonalization (solid colored lines), and comparison to theoretical $I^G_{S_0}(|q|)$ [$I^G_{S_1}(|q|)$] rescaled from numerical Bethe ansatz calculations [34] (dashed black lines). (c) $(I^G_{S_0}/I^G_{S_1})(|q|)$ as a function of τ compared to experimental data points (black squares). Calculations have been done for $J = 0.16$ eV.

For a quantitative comparison between theory and experiment, we introduce the ratio $(I^G_{S_0}/I^G_{S_1})(|q|,\tau)$. This is shown in Fig. 4(c), where the experimental data points (black squares) are compared to the theoretical results for different τ (solid lines). This comparison yields $\tau \approx 1.6$–2.2 fs, in good agreement with experimental estimates of the core-hole lifetime in Cu L_3-edge RIXS ($\Gamma \sim 0.3$–0.4 eV) [36]. This result indicates that the generation of S_0 excitations in $CaCu_2O_3$ is evidently a slow process compared to the core-hole lifetime and that the intensity of S_0 excitations scales as the dimensionless time scale ratio $\tilde{\tau} = \tau/\tau_{S_0} = J/\Gamma$. By tuning the $\tilde{\tau}$ knob, it would then be possible to investigate the time dynamics of the S_0 excitation further. This can be experimentally achieved in several ways, by controlling independently J—i.e., by considering different materials, isovalent dopings, or strain [37]—and Γ, i.e., by moving to other absorption edges.

The method presented here, using the simultaneous energy, time, and momentum resolution, goes beyond the capabilities of other time-domain approaches, e.g., laser-based or time-resolved neutron techniques. The former are limited to $q \simeq 0$, where $I^G_{S_0} = 0$, while the latter cannot access the time scale associated with S_0 excitations. On the other hand, future perspectives of RIXS experiments at XFEL facilities in stimulated-emission mode promise a continuous control of the time scale ratio $\tilde{\tau}$.

In conclusion, we have experimentally determined the contributions of single (S_1) and double (S_0) spin-flip excitations to the measured magnetic RIXS spectra of $CaCu_2O_3$. We have then isolated the corresponding S_1 and S_0 Cu L_3-edge RIXS ground-state dynamical structure factors and, by comparing to simulations of spin-excitation dynamics in a 1D $S = 1/2$ AFM system, we have found that their ratio is directly influenced by the spin dynamics within the core-hole lifetime window. In particular, we have shown that the S_1 process is essentially insensitive to changes in all relevant time scales, while the S_0 belongs to the femtosecond time scale, and its response can be modified by changing the ratio J/Γ, experimentally feasible by changing, e.g., stoichiometry, absorption edge, or strain, or by using forthcoming XFEL sources.

We acknowledge fruitful discussions with K. Wohlfeld and S. Johnston. This work was performed at the ADRESS beam line of the Swiss Light Source using the SAXES instrument jointly built by Paul Scherrer Institut, Switzerland and Politecnico di Milano, Italy. This project was supported by the Swiss National Science Foundation and its National Centre of Competence in Research MaNEP. The research leading to these results has received funding from the European Community's Seventh Framework Programme (No. FP7/2007-2013) under Grant No. 290605 (PSIFELLOW/COFUND). We gratefully acknowledge financial support through the Emmy-Noether Program (V. B., R. K., and J. G. under Grant No. GE1647/2-1, M. D. and S. K. under Grant No. DA 1235/1-1). V. B. also acknowledges the financial support of Deutscher Akademischer Austauschdienst (DAAD).

*Present address: National Synchrotron Light Source II, Brookhaven National Laboratory, Upton, New York 11973, USA.
bisogni@bnl.gov
†Present address: Fritz-Haber-Institut der Max-Planck-Gesellschaft, Faradayweg 4-6, 14195 Berlin, Germany.
‡Present address: Diamond Light Source, Harwell Science and Innovation Campus, Didcot, Oxfordshire OX11 0DE, United Kingdom.
§Present address: Department of Bioelectronics and Biosensors, Alagappa University, Karaikudi-630 003, Tamilnadu, India.

[1] B. J. Kim, H. Koh, E. Rotenberg, S.-J. Oh, H. Eisaki, N. Motoyama, S. Uchida, T. Tohyama, S. Maekawa, Z.-X. Shen, and C. Kim, Nat. Phys. **2**, 397 (2006).
[2] B. Lake, A. M. Tsvelik, S. Notbohm, D. Alan Tennant, T. G. Perring, M. Reehuis, C. Sekar, G. Krabbes, and B. Büchner, Nat. Phys. **6**, 50 (2009).
[3] J. Schlappa, K. Wohlfeld, K. J. Zhou, M. Mourigal, M. W. Haverkort, V. N. Strocov, L. Hozoi, C. Monney, S. Nishimoto, S. Singh, A. Revcolevschi, J.-S. Caux, L. Patthey, H. M. Rønnow, J. van den Brink, and T. Schmitt, Nature (London) **485**, 82 (2012).
[4] P. Emma *et al.*, Nat. Photonics **4**, 641 (2010).
[5] N. Bloembergen, Rev. Mod. Phys. **71**, S283 (1999).
[6] A. L. Cavalieri, N. Müller, T. Uphues, V. S. Yakovlev, A. Baltuska, B. Horvath, B. Schmidt, L. Blümel, R. Holzwarth, S. Hendel, M. Drescher, U. Kleineberg, P. M. Echenique, R. Kienberger, F. Krausz, and U. Heinzmann, Nature (London) **449**, 1029 (2007).
[7] F. Krausz, Rev. Mod. Phys. **81**, 163 (2009).
[8] P. A. Brühwiler, O. Karis, and N. Mårtensson, Rev. Mod. Phys. **74**, 703 (2002).
[9] P. Skytt, P. Glans, J.-H. Guo, K. Gunnelin, C. Såthe, J. Nordgren, F. K. Gel'mukhanov, A. Cesar, and H. Ågren, Phys. Rev. Lett. **77**, 5035 (1996).
[10] A. Föhlisch, Appl. Phys. A **85**, 351 (2006).
[11] L. Braicovich and G. van der Laan, Phys. Rev. B **78**, 174421 (2008).
[12] A. Pietzsch, Y.-P. Sun, F. Hennies, Z. Rinkevicius, H. O. Karlsson, T. Schmitt, V. N. Strocov, J. Andersson, B. Kennedy, J. Schlappa, A. Föhlisch, J.-E. Rubensson, and F. Gel'mukhanov, Phys. Rev. Lett. **106**, 153004 (2011).
[13] J. P. Hill, G. Blumberg, Y. J. Kim, D. S. Ellis, S. Wakimoto, R. J. Birgeneau, S. Komiya, Y. Ando, B. Liang, R. L. Greene, D. Casa, and T. Gog, Phys. Rev. Lett. **100**, 097001 (2008).
[14] L. Braicovich, L. J. P. Ament, V. Bisogni, F. Forte, C. Aruta, G. Balestrino, N. B. Brookes, G. M. De Luca, P. G. Medaglia, F. Miletto Granozio, M. Radovic, M. Salluzzo, J. van den Brink, and G. Ghiringhelli, Phys. Rev. Lett. **102**, 167401 (2009).
[15] J. Schlappa, T. Schmitt, F. Vernay, V. N. Strocov, V. Ilakovac, B. Thielemann, H. M. Rønnow, S. Vanishri, A. Piazzalunga, X. Wang, L. Braicovich, G. Ghiringhelli, C. Marin, J. Mesot, B. Delley, and L. Patthey, Phys. Rev. Lett. **103**, 047401 (2009).
[16] L. Braicovich, J. van den Brink, V. Bisogni, M. M. Sala, L. J. P. Ament, N. B. Brookes, G. M. De Luca, M. Salluzzo, T. Schmitt, V. N. Strocov, and G. Ghiringhelli, Phys. Rev. Lett. **104**, 077002 (2010).
[17] M. Guarise, B. Dalla Piazza, M. Moretti Sala, G. Ghiringhelli, L. Braicovich, H. Berger, J. N. Hancock, D. van der Marel, T. Schmitt, V. N. Strocov, L. J. P. Ament, J. van den Brink, P.-H. Lin, P. Xu, H. M. Rønnow, and M. Grioni, Phys. Rev. Lett. **105**, 157006 (2010).
[18] L. J. P. Ament, M. van Veenendaal, T. P. Devereaux, J. P. Hill, and J. van den Brink, Rev. Mod. Phys. **83**, 705 (2011).
[19] M. P. M. Dean, R. S. Springell, C. Monney, K. J. Zhou, J. Pereiro, I. Božović, B. Dalla Piazza, H. M. Ronnøw, E. Morenzoni, J. van den Brink, T. Schmitt, and J. P. Hill, Nat. Mater. **11**, 850 (2012).
[20] L. J. P. Ament, G. Ghiringhelli, M. M. Sala, L. Braicovich, and J. van den Brink, Phys. Rev. Lett. **103**, 117003 (2009).
[21] S. Kourtis, J. van den Brink, and M. Daghofer, Phys. Rev. B **85**, 064423 (2012).
[22] V. Bisogni, L. Simonelli, L. J. P. Ament, F. Forte, M. Moretti Sala, M. Minola, S. Huotari, J. van den Brink, G. Ghiringhelli, N. B. Brookes, and L. Braicovich, Phys. Rev. B **85**, 214527 (2012).
[23] V. N. Strocov, T. Schmitt, U. Flechsig, T. Schmidt, A. Imhof, Q. Chen, J. Raabe, R. Betemps, D. Zimoch, J. Krempasky, A. Piazzalunga, X. Wang, M. Grioni, and L. Patthey, J. Synchrotron Radiat. **17**, 631 (2010).
[24] G. Ghiringhelli, A. Piazzalunga, C. Dallera, G. Trezzi, L. Braicovich, T. Schmitt, V. N. Strocov, R. Betemps, L. Patthey, X. Wang, and M. Grioni, Rev. Sci. Instrum. **77**, 113108 (2006).
[25] C. Sekar, G. Krabbes, and A. Teresiak, J. Cryst. Growth **273**, 403 (2005).
[26] E. Bordas, C. de Graaf, R. Caballol, and C. J. Calzado, Phys. Rev. B **71**, 045108 (2005).
[27] I. A. Zaliznyak, H. Woo, T. G. Perring, C. L. Broholm, C. D. Frost, and H. Takagi, Phys. Rev. Lett. **93**, 087202 (2004).
[28] V. Kiryukhin, Y. J. Kim, K. J. Thomas, F. C. Chou, R. W. Erwin, Q. Huang, M. A. Kastner, and R. J. Birgeneau, Phys. Rev. B **63**, 144418 (2001).
[29] M. W. Haverkort, Phys. Rev. Lett. **105**, 167404 (2010).
[30] L. Braicovich, M. Moretti Sala, L. J. P. Ament, V. Bisogni, M. Minola, G. Balestrino, D. Di Castro, G. M. De Luca, M. Salluzzo, G. Ghiringhelli, and J. van den Brink, Phys. Rev. B **81**, 174533 (2010).
[31] M. Moretti Sala, V. Bisogni, C. Aruta, G. Balestrino, H. Berger, N. B. Brookes, G. M. De Luca, D. Di Castro,

M. Grioni, M. Guarise, P. G. Medaglia, F. Miletto Granozio, M. Minola, P. Perna, M. Radovic, M. Salluzzo, T. Schmitt, K. J. Zhou, L. Braicovich, and G. Ghiringhelli, New J. Phys. **13**, 043026 (2011).

[32] See Supplemental Material at http://link.aps.org/supplemental/10.1103/PhysRevLett.112.147401 for the S_0/S_1 extrapolation from the experimental data and details about the theoretical modeling of the RIXS cross section, which includes Refs. [38–47].

[33] J. I. Igarashi and T. Nagao, Phys. Rev. B **85**, 064422 (2012).

[34] A. Klauser, J. Mossel, J.-S. Caux, and J. van den Brink, Phys. Rev. Lett. **106**, 157205 (2011).

[35] M. A. van Veenendaal, H. Eskes, and G. A. Sawatzky, Phys. Rev. B **47**, 11462 (1993).

[36] R. Nyholm, N. Mårtensson, A. Lebugle, and U. Axelsson, J. Phys. F **11**, 1727 (1981); F. Al Shamma, M. Abbate, and J. C. Fuggle, in *Unoccupied Electronic States: Fundamentals for XANES, EELS, IPS and BIS*, edited by J. C. Fuggle and J. E. Inglesfield, Topics in Applied Physics Vol. 69 (Springer-Verlag, Berlin, 1992), pp. 347–351.

[37] M. Minola, D. Di Castro, L. Braicovich, N. B. Brookes, D. Innocenti, M. Moretti Sala, A. Tebano, G. Balestrino, and G. Ghiringhelli, Phys. Rev. B **85**, 235138 (2012).

[38] J. Sakurai, *Advanced Quantum Mechanics*, Addison-Wesley Series in Advanced Physics (Addison-Wesley, Reading, MA, 1967).

[39] G. van der Laan, C. Westra, C. Haas, and G. A. Sawatzky, Phys. Rev. B **23**, 4369 (1981).

[40] A. Fujimori, E. Takayama-Muromachi, Y. Uchida, and B. Okai, Phys. Rev. B **35**, 8814 (1987).

[41] Z.-X. Shen, J. W. Allen, J. J. Yeh, J.-S. Kang, W. Ellis, W. Spicer, I. Lindau, M. B. Maple, Y. D. Dalichaouch, M. S. Torikachvili, J. Z. Sun, and T. H. Geballe, Phys. Rev. B **36**, 8414 (1987).

[42] K. Okada and A. Kotani, J. Phys. Soc. Jpn. **58**, 2578 (1989).

[43] K. Okada and A. Kotani, Phys. Rev. B **52**, 4794 (1995).

[44] K. Okada, A. Kotani, K. Maiti, and D. D. Sarma, J. Phys. Soc. Jpn. **65**, 1844 (1996).

[45] K. Okada and A. Kotani, J. Electron Spectrosc. Relat. Phenom. **86**, 119 (1997).

[46] T. Mizokawa, T. Konishi, A. Fujimori, Z. Hiroi, M. Takano, and Y. Takeda, J. Electron Spectrosc. Relat. Phenom. **92**, 97 (1998).

[47] K. Okada, J. Phys. Soc. Jpn. **78**, 034725 (2009).